International Journal of Mathematics and
Computer Applications Research (IJMCAR)
ISSN(P): 2249-6955; ISSN(E): 2249-8060
Vol. 7, Issue 2, Apr 2017, 1-22

HALL CURRENT EFFECTS ON MHD FREE CONVECTIVE HEAT AND MASS TRANSFER FLOW PAST AN OSCILLATING VERTICAL POROUS PLATE IN THE PRESENCE OF RADIATION, THERMAL & MASS DIFFUSION WITH CHEMICAL REACTION

D. BABU REDDY & G. S. S. RAJU

Department of Mathematics, JNTUA College of Engineering, Pulivendula, Andhra Pradesh, India

ABSTRACT

A boundary layer analysis has been presented to study the effects of rotation, Soret and Hall current on the hydromagnetic natural convection and mass transfer flow of a viscous, incompressible, Newtonian, chemically reacting and optically thin gray radiating fluid past along a vertical oscillating plate with variable temperature and mass diffusion in the presence of transverse magnetic field. It is assumed that the entire system rotates with a uniform angular velocity Ω about the normal to the plate. The dimensionless governing equations are solved by Laplace transform technique and solutions for primary velocity, secondary velocity, temperature and concentration field are obtained. The expressions for skin friction, Nusselt number and Sherwood number are also obtained.

KEYWORDS: Hall Current, Rotation, Soret Effect, MHD, Free Convection, Porous Medium, Schmidt Number

Received: Jan 15, 2017; **Accepted:** Feb 27, 2017; **Published:** Mar 01, 2017; **Paper Id.:** IJMCARAPR20171

Original Article

1. INTRODUCTION

Natural convective and heat transfer flows through a porous medium under the influence of a magnetic field has attracted a great deal of attention from researchers because of its possible applications in many branches of both nature and technology, such as its applications in transportation cooling of re-entry vehicles and rocket boosters, cross-hatching on ablative surfaces and film vaporization in combustion chambers. In recent years, the study on a flow through a porous medium has various applications encountered in engineering and geophysical viz. in the agricultural engineering, to study the underground water through canals, filtration and refinement process in the chemical engineering; to study the motion of natural gas in the petroleum technology, water and oil through the oil reservoirs. In sight of these applications, many researchers have studied hydro magnetic natural convection and mass transfer flow in a porous medium with different configurations; Noticeable among them are [1-4]. From all these studies, they obtained a numerical solution to the problem of an unsteady flow past an infinite vertical plate embedded in a porous medium with oscillating plate temperature subjected to a constant suction. Raptis and Perdikis [5] have presented a study on unsteady flow through a highly porous medium in the presence of radiation. Ahmed [6] investigated the influence of transverse periodic permeability oscillating with time on the heat transfer flow of a viscous incompressible fluid past an infinite vertical porous plate embedded in a highly porous medium subjected to a periodic suction velocity. Kumar and Verma [7] investigated an unsteady flow past an infinite vertical permeable plate with oscillating plate temperature in the presence of constant suction.

Radiation effects on the boundary layer play a vital role, in controlling heat transfer, in such cases the effect of thermal radiation or mass diffusion one has taken into account. Mahmoud and Chamkha [8] have presented the effects of a radiation on natural convection flow of a Newtonian fluid along a vertical surface embedded in a porous medium. Natural convection flow of an optically thin gray gas past a semi-infinite vertical plate in the presence of chemical reaction was investigated by Soundalgekar and Takhar [9]. Hossain and Takhar [10] have considered the effects of radiation on mixed convection flow along an isothermal vertical plate. In all the above studies, the vertical plate has been considered as stationary. Raptis and Perdikis [11] investigated the influence of thermal radiation and free convection flow past a moving vertical plate. An analytical method was employed to solve the governing equations. Ahmed [12] have presented MHD flow of steady mixed convective heat and mass transfer flow of an optically thin gray gas over an infinite vertical porous plate with constant suction by considering the effects of radiation and magnetic Prandtl number. Ahmed and Kalita [13] studied the effects of porosity and MHD flow of a viscous incompressible electrically conducting fluid through a porous medium on a horizontal channel in the presence of thermal radiation and transverse magnetic field. Ahmed and Kalita [14] have studied the combined effects of chemical reaction and magnetic field on the convective and mass transfer of Newtonian fluids over an infinite vertical oscillating plate in the presence of variable mass diffusion. Ahmed et al. [15] obtained a numerical solution for the problem of MHD free convective and mass transfer flow past an impulsively started semi-infinite vertical plate in the presence of thermal radiation by using an implicit finite-difference scheme of Crank–Nicolson type. Ahmed et al. [16] were examined the effects of Darcian drag force and conduction on the unsteady two-dimensional hydromagnetic flow of a viscous, electrically conducting, radiative and Newtonian fluid over a vertical plate adjacent to a Darcian regime in the existence of thermal radiation. Ahmed [17] analyzed the influence of radiation-conduction, porosity of the porous medium and chemical reaction on the unsteady MHD free convection flow past a semi-infinite vertical plate in the presence of thermal radiation. An implicit finite-difference scheme of the Crank–Nicolson type is employed to solve the boundary layer equations. We obtained the results which are efficient, accurate, extensively validated and unconditionally stable. Recently Ahmed et al. [18] were presented the analytical and numerical solution for the problem of MHD laminar boundary flow of Newtonian fluid along a vertical oscillating plate in a porous medium with mass diffusion in the influence of thermal radiation.

The objective of the Present communication is to extend the work of Ahmed [18] into three directions. Firstly to consider the three-dimensional flow of Newtonian fluid. Effects of rotation, Soret and Hall current are present. Secondly to analyze the behavior of variable magnetic field under low Reynolds number assumption. Thirdly to compute the analytical solutions through Laplace transform technique and the effects of various parameters are discussed numerically and graphically.

2. FORMULATION OF THE PROBLEM

We consider the unsteady hydromagnetic natural convection and mass transfer flow of a viscous, incompressible, Newtonian, chemically reacting and optically thin gray radiating fluid past along a vertical oscillating plate immersed in a saturated porous medium in a rotating system taking Hall current and Soret effects into account. Assuming Hall currents, then the Ohm's law may be put in the following form:

$$\vec{j} = \frac{\sigma}{1+m^2}(\vec{E}+\vec{V}\times\vec{B}-\frac{1}{\sigma n_e}\vec{j}\times\vec{B}),$$

where $\vec{V}$ represents the velocity vector,$\vec{E}$ is the intensity vector of the electric field, $\vec{B}$ is the magnetic induction vector, $\vec{J}$ the electric current density vector, m is the Hall current parameter, σ the electrical conductivity and n_e is the number density of the electron. An interesting fact that the flow becomes three-dimensional due to the Hall current effect, which gives rise to a cross flow in the $\bar{y}$- direction.

The Cartesian coordinate system is chosen in such a way that $\bar{x}$-axis is considered along the plate in upward direction and $\bar{z}$-axis normal to plane of the plate in the fluid. A uniform transverse magnetic field B_0 is applied in the $\bar{z}$ - direction. The fluid and plate rotate in anticlockwise direction with uniform angular velocity Ω about $\bar{z}$-axis. At time $\bar{t} \leq 0$, both the plate and fluid are at rest and are maintained at a uniform temperature $\bar{T}_\infty$ and species concentration $\bar{C}_\infty$ at the surface of the plate as well as at every point within the fluid. At time $\bar{t} > 0$, plate starts moving in $\bar{x}$-direction with a velocity $\bar{u} = u_0 \cos(\bar{\omega}\bar{t})$ in its own plane. At the same time the temperature of the plate is raised to $\bar{T}_\infty + (\bar{T}_w - \bar{T}_\infty)A\bar{t}$ and species concentration at the surface of the plate is raised to $\bar{C}_\infty + (\bar{C}_w - \bar{C}_\infty)\, A\bar{t}$ and is maintained thereafter. The sketch of the fluid model as presented in Figure 1.

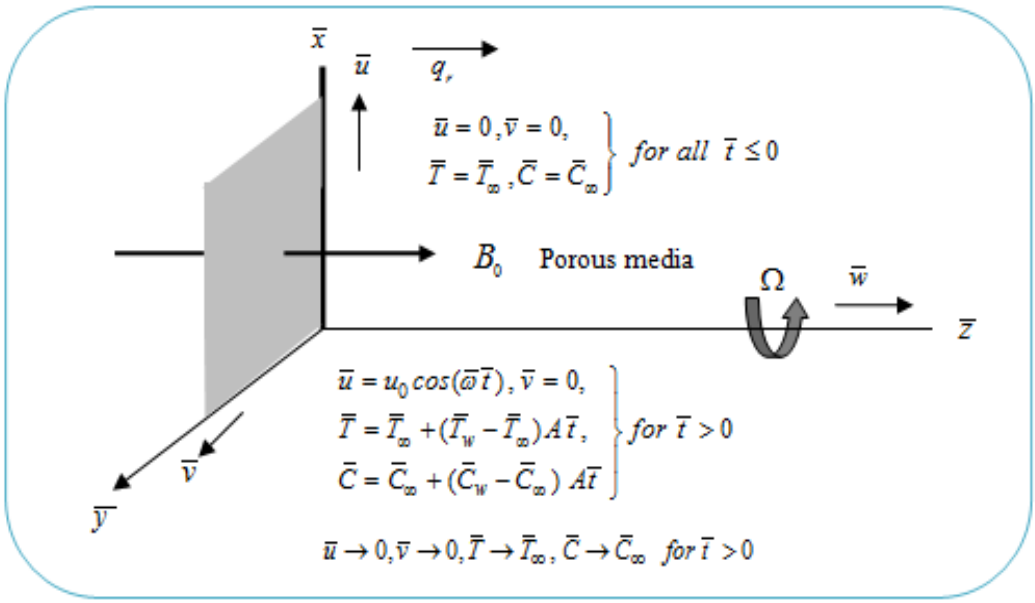

Figure 1: Geometry of the Problem

Since the plate is of infinite extent in $\bar{x}$ and $\bar{y}$ directions and is electrically non-conducting, then all the flow variables in the problem except pressure are functions of $\bar{z}$ and $\bar{t}$ alone. The effect of polarization of fluid is negligible because there is no applied or polarized voltages exist on fluid flow. In such case, no energy is added or extracted from the fluid by electrically. It is assumed that the Induced magnetic field due to the flow is neglected compared to the applied magnetic field. This assumption is physically justified for liquid metals and partially ionized fluids which are commonly used in industrial applications, because their magnetic Reynolds number is very small.

Under the above stated assumptions and usual Boussinesq's approximation, the governing equations of the flow are:

$$\frac{\partial \bar{u}}{\partial \bar{t}} + 2\Omega\bar{v} = \upsilon\frac{\partial^2 \bar{u}}{\partial \bar{z}^2} - \frac{\sigma B_0^2}{\rho(1+m^2)}(\bar{u} + m\bar{v}) + g\beta(\bar{T} - \bar{T}_\infty) + g\bar{\beta}(\bar{C} - \bar{C}_\infty) - \frac{\upsilon\bar{u}}{\bar{K}r} \tag{1}$$

$$\frac{\partial \bar{v}}{\partial \bar{t}} - 2\Omega\bar{u} = \upsilon\frac{\partial^2 \bar{v}}{\partial \bar{z}^2} + \frac{\sigma B_0^2}{\rho(1+m^2)}(m\bar{u} - \bar{v}) - \frac{\upsilon\bar{v}}{\bar{K}r} \tag{2}$$

$$\rho Cp\frac{\partial \bar{T}}{\partial \bar{t}} = k\frac{\partial^2 \bar{T}}{\partial \bar{z}^2} - \frac{\partial q_r}{\partial \bar{z}} - \bar{Q}(\bar{T} - \bar{T}_\infty) \tag{3}$$

$$\frac{\partial \bar{C}}{\partial \bar{t}} = D_M\frac{\partial^2 \bar{C}}{\partial \bar{z}^2} + D_T\frac{\partial^2 \bar{T}}{\partial \bar{z}^2} - \bar{C}_r(\bar{C} - \bar{C}_\infty) \tag{4}$$

where $\bar{u}$, $\bar{v}$ and $\bar{w}$ denote the velocity components of the fluid in the $\bar{x}$, $\bar{y}$ and $\bar{z}$ directions respectively, υ is the kinematic viscosity, σ is the fluid density, ρ is the electrical conductivity, $m = \omega_e\tau_e$ is the Hall parameter, ω_e is the cyclotron frequency, τ_e is the electron collision time, g is the acceleration due to gravity, β is the volumetric coefficient of thermal expansion, $\bar{\beta}$ is the volumetric coefficient of concentration expansion, $\bar{K}_r$ is the permeability of the porous medium, C_p specific heat at constant pressure, $\bar{T}$ is the temperature of the fluid, $\bar{C}$ is the species concentration, k is the thermal conductivity, q_r is the radiative heat flux , D_M is the coefficient of mass diffusivity, D_T is the thermal diffusion ratio and $\bar{C}_r$ is the chemical reaction parameter.

The Initial and boundary conditions for the fluid flow are given below:

$$\left.\begin{array}{ll} \bar{t} \le 0: \ \bar{u} = 0, \bar{v} = 0, \bar{T} = \bar{T}_\infty, \ \bar{C} = \bar{C}_\infty & \text{for all } \bar{z} \\ \bar{t} > 0: \ \bar{u} = u_0\cos(\bar{\omega}\bar{t}), \ \bar{v} = 0, \ \bar{T} = \bar{T}_\infty + (\bar{T}_w - \bar{T}_\infty)A\bar{t}, \bar{C} = \bar{C}_\infty + (\bar{C}_w - \bar{C}_\infty)A\bar{t} & \text{at } \bar{z} = 0 \\ \bar{t} > 0: \ \bar{u} \to 0, \ \bar{v} \to 0, \ \bar{T} \to \bar{T}_\infty, \ \bar{C} \to \bar{C}_\infty & \text{as } \bar{z} \to \infty \end{array}\right\} \tag{5}$$

The local radiant absorption for the case of an optically thin gray gas is expressed as

$$\frac{\partial q_r}{\partial \bar{z}} = -4\,\bar{a}\,\bar{\sigma}(\bar{T}_\infty^4 - \bar{T}^4) \tag{6}$$

where $\bar{a}$ and $\bar{\sigma}$ are the Mean absorption coefficient and the Stefan-Boltzmann constant, respectively. The temperature difference within the flow is assumed to be sufficiently small, then Eq. (6) can be linearized by expanding into the Taylor series about $\bar{T}_\infty$, which after neglecting the higher order terms. This results the following approximation:

$$\bar{T}^4 = 4\bar{T}_\infty^3\bar{T} - 3\bar{T}_\infty^4 \tag{7}$$

By use of Eqs. (6) and (7) in Eqs. (3), reduces into the following form:

$$\rho Cp\frac{\partial \bar{T}}{\partial \bar{t}} = k\frac{\partial^2 \bar{T}}{\partial \bar{z}^2} - 16\,\bar{a}\,\bar{\sigma}\bar{T}_\infty^3(\bar{T} - \bar{T}_\infty) - \bar{Q}(\bar{T} - \bar{T}_\infty) \tag{8}$$

We introduce the following non-dimensional quantities

$$u=\frac{\bar{u}}{u_0}, v=\frac{\bar{v}}{u_0}, \theta=\frac{\bar{T}-\bar{T}_\infty}{\bar{T}_w-\bar{T}_\infty}, \varphi=\frac{\bar{C}-\bar{C}_\infty}{\bar{C}_w-\bar{C}_\infty}, t=\frac{\bar{t}\,u_0^2}{\upsilon}, z=\frac{\bar{z}\,u_0}{\upsilon}, A=\frac{u_0^2}{\upsilon}, \omega=\frac{\bar{\omega}\,\upsilon}{u_0^2} \tag{9}$$

With the help of above dimensionless variables, Eqs (1), (2), (4) and (8) yields

$$\frac{\partial u}{\partial t}+2K^2 v=\frac{\partial^2 u}{\partial z^2}-\frac{M}{\left(1+m^2\right)}(u+mv)+Gr\,\theta+Gm\,\varphi-\frac{u}{Kr} \tag{10}$$

$$\frac{\partial v}{\partial t}-2K^2 u=\frac{\partial^2 v}{\partial z^2}+\frac{M}{\left(1+m^2\right)}(mu-v)-\frac{v}{Kr} \tag{11}$$

$$\frac{\partial \theta}{\partial t}=\frac{1}{\Pr}\frac{\partial^2 \theta}{\partial z^2}-\left(\frac{R}{\Pr}+Q\right)\theta \tag{12}$$

$$\frac{\partial \phi}{\partial t}=\frac{1}{Sc}\frac{\partial^2 \phi}{\partial z^2}+Sr\frac{\partial^2 \theta}{\partial z^2}-Cr\,\phi \tag{13}$$

Where K^2 is the rotation parameter, M denotes the magnetic parameter, Gr stands for thermal Grash of number, Gm stands for solutal Grashof number, Kr is the permeability parameter, Pr is the Prandtl number, R is the radiation parameter, Q is the heat source parameter, Sc is the Schmidt number, Sr is the Soret number and Cr is the chemical reaction parameter as follows:

$$K^2=\frac{\Omega\upsilon}{u_0^2}, M=\frac{\sigma B_0^2\,\upsilon}{\rho u_0^2}, Gr=\frac{g\beta\upsilon(\bar{T}_w-\bar{T}_\infty)}{u_0^3}, Gm=\frac{g\bar{\beta}\upsilon(\bar{C}_w-\bar{C}_\infty)}{u_0^3}, Kr=\frac{\overline{Kr}\,u_0^2}{\upsilon^2}$$

$$\Pr=\frac{\upsilon\rho Cp}{k}, R=\frac{16\,\bar{a}\,\bar{\sigma}\,\upsilon^2\bar{T}_\infty^3}{k\,u_0^2}, Q=\frac{\bar{Q}\,\upsilon}{\rho Cp\,u_0^2}, Sc=\frac{\upsilon}{D_M}, Sr=\frac{D_T(\bar{T}_w-\bar{T}_\infty)}{\upsilon(\bar{C}_w-\bar{C}_\infty)}, Cr=\frac{\bar{C}_r\,\upsilon}{u_0^2}\ .$$

The corresponding initial and boundary conditions are given by:

$$\left.\begin{array}{lll} t\le 0: & u=0, v=0, \theta=0, & \phi=0 \quad \text{for all } z \\ t>0: & u=\cos(\omega t), & v=0, \quad \theta=t, \quad \phi=t \quad \text{at} \quad z=0 \\ t>0: & u\to 0, & v\to 0, \quad \theta\to 0, \quad \phi\to 0 \quad \text{as} \quad z\to\infty \end{array}\right\} \tag{14}$$

Combining equations (10) and (11), we obtain

$$\frac{\partial F}{\partial t}=\frac{\partial^2 F}{\partial z^2}-N\,F+Gr\,\theta+Gm\,\phi \tag{15}$$

Where $F = u + iv$ *and* $N = \frac{M(1-im)}{(1+m^2)} + \frac{1}{Kr} - 2iK^2$

The initial and boundary conditions (14), in compact form becomes

$$\left.\begin{array}{ll} t \le 0 : F = 0, \theta = 0, \ \varphi = 0 & \text{for all } z \\ t > 0 : F = \cos(\omega t), \ \theta = t, \ \phi = t & \text{at } z = 0 \\ t > 0 : F \to 0, \ \theta \to 0, \ \phi \to 0 & \text{as } z \to \infty \end{array}\right\} \tag{16}$$

3. SOLUTION OF THE PROBLEM

The set of Eqs. (12), (13) and (15) subject to the initial and boundary conditions (16) are solved analytically with the help of Laplace transform technique. The exact solutions for the fluid temperature θ (z, t) species concentration ϕ(z, t) and fluid velocity F (z, t) are obtained and expressed in the following form:

$$\theta(z,t) = \left(\frac{t}{2} - \frac{z\,\mathrm{Pr}}{4\sqrt{S}}\right)\exp\left(-z\sqrt{S}\right)erfc\left(\eta\sqrt{\mathrm{Pr}} - \sqrt{St/\mathrm{Pr}}\right) + \left(\frac{t}{2} + \frac{z\,\mathrm{Pr}}{4\sqrt{S}}\right)\exp\left(z\sqrt{S}\right)erfc\left(\eta\sqrt{\mathrm{Pr}} + \sqrt{St/\mathrm{Pr}}\right) \tag{17}$$

$$\phi(z,t) = A_6\left\{\left(\frac{t}{2} - \frac{z}{4}\sqrt{\frac{Sc}{Cr}}\right)\exp\left(-z\sqrt{ScCr}\right)erfc\left[\eta\sqrt{Sc} - \sqrt{Crt}\right] + \left(\frac{t}{2} + \frac{z}{4}\sqrt{\frac{Sc}{Cr}}\right)\exp\left(z\sqrt{ScCr}\right)erfc\left[\eta\sqrt{Sc} + \sqrt{Crt}\right]\right\}$$

$$-\frac{A_5}{2}\left\{\exp\left(-z\sqrt{ScCr}\right)erfc\left[\eta\sqrt{Sc} - \sqrt{Crt}\right] + \exp\left(z\sqrt{ScCr}\right)erfc\left[\eta\sqrt{Sc} + \sqrt{Crt}\right]\right\}$$

$$+\frac{A_5\exp(-A_2t)}{2}\left\{\exp\left(-z\sqrt{Sc}\sqrt{Cr - A_2}\right)erfc\left[\eta\sqrt{Sc} - \sqrt{(Cr - A_2)t}\right] + \exp\left(z\sqrt{Sc}\sqrt{Cr - A_2}\right)erfc\left[\eta\sqrt{Sc} + \sqrt{(Cr - A_2)t}\right]\right\}$$

$$+A_4\left\{\left(\frac{t}{2} - \frac{z}{4}\sqrt{\frac{\mathrm{Pr}}{B}}\right)\exp\left(-z\sqrt{B\,\mathrm{Pr}}\right)erfc\left[\eta\sqrt{\mathrm{Pr}} - \sqrt{Bt}\right] + \left(\frac{t}{2} + \frac{z}{4}\sqrt{\frac{\mathrm{Pr}}{B}}\right)\exp\left(z\sqrt{B\,\mathrm{Pr}}\right)erfc\left[\eta\sqrt{\mathrm{Pr}} + \sqrt{Bt}\right]\right\}$$

$$+\frac{A_5}{2}\left\{\exp\left(-z\sqrt{B\,\mathrm{Pr}}\right)erfc\left[\eta\sqrt{\mathrm{Pr}} - \sqrt{Bt}\right] + \exp\left(z\sqrt{BP_r}\right)erfc\left[\eta\sqrt{\mathrm{Pr}} + \sqrt{Bt}\right]\right\}$$

$$-\frac{A_5\exp(-A_2t)}{2}\left\{\exp\left(-z\sqrt{\mathrm{Pr}}\sqrt{B - A_2}\right)erfc\left[\eta\sqrt{\mathrm{Pr}} - \sqrt{(B - A_2)t}\right] + \exp\left(z\sqrt{\mathrm{Pr}}\sqrt{B - A_2}\right)erfc\left[\eta\sqrt{\mathrm{Pr}} + \sqrt{(B - A_2)t}\right]\right\} \tag{18}$$

$$F(z,t) = \frac{\exp(i\omega t)}{4}\left[\exp\left(-z\sqrt{N + i\omega}\right)erfc\left(\eta - \sqrt{(N + i\omega)t}\right) + \exp\left(z\sqrt{N + i\omega}\right)erfc\left(\eta + \sqrt{(N + i\omega)t}\right)\right]$$

$$+\frac{\exp(-i\omega t)}{4}\left[\exp\left(-z\sqrt{N - i\omega}\right)erfc\left(\eta - \sqrt{(N - i\omega)t}\right) + \exp\left(z\sqrt{N - i\omega}\right)erfc\left(\eta + \sqrt{(N - i\omega)t}\right)\right]$$

$$+\frac{A_{27}}{2}\left[\exp\left(-z\sqrt{N}\right)erfc\left(\eta - \sqrt{Nt}\right) + \exp\left(z\sqrt{N}\right)erfc\left(\eta + \sqrt{Nt}\right)\right]$$

$$+\frac{A_{28}\exp(-A_8t)}{2}\left[\exp\left(-z\sqrt{N - A_8}\right)erfc\left(\eta - \sqrt{(N - A_8)t}\right) + \exp\left(z\sqrt{N - A_8}\right)erfc\left(\eta + \sqrt{(N - A_8)t}\right)\right]$$

$$+\frac{A_{29}\exp(-A_2t)}{2}\left[\exp\left(-z\sqrt{N-A_2}\right)erfc\left(\eta-\sqrt{(N-A_2)t}\right)+\exp\left(z\sqrt{N-A_2}\right)erfc\left(\eta+\sqrt{(N-A_2)t}\right)\right]$$

$$+\frac{A_{30}\exp(-A_{10}t)}{2}\left[\exp\left(-z\sqrt{N-A_{10}}\right)erfc\left(\eta-\sqrt{(N-A_{10})t}\right)+\exp\left(z\sqrt{N-A_{10}}\right)erfc\left(\eta+\sqrt{(N-A_{10})t}\right)\right]$$

$$+A_{31}\left[\left(\frac{t}{2}-\frac{z\,\mathrm{Pr}}{4\sqrt{S}}\right)\exp\left(-z\sqrt{S}\right)erfc\left(\eta\sqrt{\mathrm{Pr}}-\sqrt{\frac{St}{\mathrm{Pr}}}\right)+\left(\frac{t}{2}+\frac{z\,\mathrm{Pr}}{4\sqrt{S}}\right)\exp\left(z\sqrt{S}\right)erfc\left(\eta\sqrt{\mathrm{Pr}}+\sqrt{\frac{St}{\mathrm{Pr}}}\right)\right]$$

$$+\frac{A_{32}}{2}\left[\exp\left(-z\sqrt{B\,\mathrm{Pr}}\right)erfc\left(\eta\sqrt{\mathrm{Pr}}-\sqrt{Bt}\right)+\exp\left(z\sqrt{B\,\mathrm{Pr}}\right)erfc\left(\eta\sqrt{\mathrm{Pr}}+\sqrt{Bt}\right)\right]$$

$$+\frac{A_{33}\exp(-A_8t)}{2}\left[\exp\left(-z\sqrt{\mathrm{Pr}}\sqrt{B-A_8}\right)erfc\left[\eta\sqrt{\mathrm{Pr}}-\sqrt{(B-A_8)t}\right]+\exp\left(z\sqrt{\mathrm{Pr}}\sqrt{B-A_8}\right)erfc\left[\eta\sqrt{\mathrm{Pr}}+\sqrt{(B-A_8)t}\right]\right.$$

$$\left.-\frac{A_{19}\exp(-A_2t)}{2}\left[\exp\left(-z\sqrt{\mathrm{Pr}}\sqrt{B-A_2}\right)erfc\left[\eta\sqrt{\mathrm{Pr}}-\sqrt{(B-A_2)t}\right]+\exp\left(z\sqrt{\mathrm{Pr}}\sqrt{B-A_2}\right)erfc\left[\eta\sqrt{\mathrm{Pr}}-\sqrt{(B-A_2)t}\right]\right]\right.$$

$$+A_{34}\left[\left(\frac{t}{2}-\frac{z}{4}\sqrt{\frac{Sc}{Cr}}\right)\exp\left(-z\sqrt{ScCr}\right)erfc\left[\eta\sqrt{Sc}-\sqrt{Crt}\right]+\left(\frac{t}{2}+\frac{z}{4}\sqrt{\frac{Sc}{Cr}}\right)\exp\left(z\sqrt{ScCr}\right)erfc\left[\eta\sqrt{Sc}+\sqrt{Crt}\right]\right]$$

$$+\frac{A_{35}}{2}\left[\exp\left(-z\sqrt{ScCr}\right)erfc\left[\eta\sqrt{Sc}-\sqrt{Crt}\right]+\exp\left(z\sqrt{ScCr}\right)erfc\left[\eta\sqrt{Sc}+\sqrt{Crt}\right]\right]$$

$$+\frac{A_{36}\exp(-A_{10}t)}{2}\left[\begin{array}{l}\exp\left(-z\sqrt{Sc}\sqrt{Cr-A_{10}}\right)erfc\left[\eta\sqrt{Sc}-\sqrt{(Cr-A_{10})t}\right]\\ \qquad+\exp\left(z\sqrt{Sc}\sqrt{Cr-A_{10}}\right)erfc\left[\eta\sqrt{Sc}+\sqrt{(Cr-A_{10})t}\right]\end{array}\right]$$

$$+\frac{A_{25}\exp(-A_2t)}{2}\left[\begin{array}{l}\exp\left(-z\sqrt{Sc(Cr-A_2)}\right)erfc\left[\eta\sqrt{Sc}-\sqrt{(Cr-A_2)t}\right]\\ \qquad+\exp\left(z\sqrt{Sc(Cr-A_2)}\right)erfc\left[\eta\sqrt{Sc}+\sqrt{(Cr-A_2)t}\right]\end{array}\right] \tag{19}$$

3.1. Skin Friction, Nusselt Number and Sherwood Number of the Plate

The expressions for primary skin friction τ_x, secondary skin friction τ_y, Nusselt number *Nu*, and Sherwood number *Sh*, which are measures of shear stress at the plate due to primary flow, shear stress at the plate due to secondary flow, rate of heat transfer at the plate and rate of mass transfer at the plate respectively, are presented in the following form:

$$Nu=-\left.\frac{\partial\theta}{\partial z}\right|_{z=0}=\sqrt{\frac{\mathrm{Prt}}{\pi}}\exp\left(-\sqrt{\frac{St}{\mathrm{Pr}}}\right)-\left(\frac{\mathrm{t}\sqrt{S}}{2}+\frac{\mathrm{Pr}}{4\sqrt{S}}\right)\left(erfc\left(\sqrt{\frac{St}{\mathrm{Pr}}}\right)-erfc\left(-\sqrt{\frac{St}{\mathrm{Pr}}}\right)\right) \tag{20}$$

$$Sh=\left.\frac{\partial\phi}{\partial z}\right|_{z=0}=-A_4\sqrt{\frac{\mathrm{Pr}\,t}{\pi}}\exp(-Bt)+\frac{A_4t\sqrt{B\,\mathrm{Pr}}}{2}\left[erfc(\sqrt{Bt})-erfc(-\sqrt{Bt})\right]+B_1\left[erfc(\sqrt{Bt})-erfc(-\sqrt{Bt})\right]$$

$$-A_6\sqrt{\frac{Sct}{\pi}}\exp(-Crt)+\frac{A_6t\sqrt{CrSc}}{2}\left[erfc(\sqrt{Crt})-erfc(-\sqrt{Crt})\right]+B_2\left[erfc(\sqrt{Crt})-erfc(-\sqrt{Crt})\right]$$

$$-B_3\left[erfc\left(\sqrt{(B-A_2)t}\right)-erfc\left(-\sqrt{(B-A_2)t}\right)\right]-B_4\left[erfc\left(\sqrt{(CR-A_2)t}\right)-erfc\left(-\sqrt{(CR-A_2)t}\right)\right] \quad (21)$$

$$\tau_x+i\tau_y=\left.\frac{\partial F}{\partial z}\right|_{z=0}=\frac{1}{2\sqrt{t}}\left[\frac{\partial F}{\partial \eta}\right]_{\eta=0}$$

$$=-\frac{A_{37}\exp(-\mathrm{Nt})}{\sqrt{\pi t}}-A_{38}\exp(-Bt)\sqrt{\frac{\mathrm{Pr}}{\pi t}}-A_{39}\exp(-Cr\,\mathrm{t})\sqrt{\frac{Sc}{\pi t}}$$

$$+\frac{\exp(\mathrm{i}\,\omega t)\sqrt{N+\mathrm{i}\omega}}{4}\left[erfc\left(\sqrt{(N+\mathrm{i}\omega)\,\mathrm{t}}\right)-erfc\left(-\sqrt{(N+\mathrm{i}\omega)\,\mathrm{t}}\right)\right]$$

$$+\frac{\exp(-\mathrm{i}\,\omega t)\sqrt{N-\mathrm{i}\omega}}{4}\left[erfc\left(\sqrt{(N-\mathrm{i}\omega)\,\mathrm{t}}\right)-erfc\left(-\sqrt{(N-\mathrm{i}\omega)\,\mathrm{t}}\right)\right]$$

$$+\frac{A_{19}\exp(-A_2t)\sqrt{\mathrm{Pr}(B-A_2)}}{2}\left[erfc\left(\sqrt{(B-A_2)t}\right)-erfc\left(-\sqrt{(B-A_2)t}\right)\right]$$

$$+\frac{A_{25}\exp(-A_2t)\sqrt{Sc(Cr-A_2)}}{2}\left[erfc\left(\sqrt{(Cr-A_2)t}\right)-erfc\left(-\sqrt{(Cr-A_2)t}\right)\right]$$

$$+\left(\frac{A_{26}\sqrt{N}t}{2}+\frac{A_{26}}{4\sqrt{N}}+\frac{A_{27}\sqrt{N}}{2}\right)\left[erfc\left(\sqrt{Nt}\right)-erfc\left(-\sqrt{Nt}\right)\right]$$

$$+\frac{A_{28}\exp(-A_8t)\sqrt{N-A_8}}{2}\left[erfc\left(\sqrt{(N-A_8)t}\right)-erfc\left(-\sqrt{(N-A_8)t}\right)\right]$$

$$+\frac{A_{29}\exp(-A_2t)\sqrt{N-A_2}}{2}\left[erfc\left(\sqrt{(N-A_2)t}\right)-erfc\left(-\sqrt{(N-A_2)t}\right)\right]$$

$$+\frac{A_{30}\exp(-A_{10}t)\sqrt{n-A_{10}}}{2}\left[erfc\left(\sqrt{(n-A_{10})t}\right)-erfc\left(-\sqrt{(n-A_{10})t}\right)\right]$$

$$+\left(\frac{A_{31}t\sqrt{B\,\mathrm{Pr}}}{2}+\frac{A_{31}}{4}\sqrt{\frac{PR}{B}}+\frac{A_{32}\sqrt{B\,\mathrm{Pr}}}{2}\right)\left[erfc\left(\sqrt{Bt}\right)-erfc\left(-\sqrt{Bt}\right)\right]$$

$$+\frac{A_{33}\exp(-A_8t)\sqrt{\mathrm{Pr}(B-A_8)}}{2}\left[erfc\left(\sqrt{(B-A_8)t}\right)-erfc\left(-\sqrt{(B-A_8)t}\right)\right]$$

$$+\left(\frac{A_{34}t\sqrt{CrSc}}{2}+\frac{A_{34}}{4}\sqrt{\frac{Sc}{Cr}}+\frac{A_{35}\sqrt{CrSc}}{2}\right)\left[erfc\left(\sqrt{Crt}\right)-erfc\left(-\sqrt{Crt}\right)\right]$$

$$+\frac{A_{36}\exp(-A_{10}t)\sqrt{Sc(Cr-A_{10})}}{2}\left[erfc\left(\sqrt{(Cr-A_{10})t}\right)-erfc\left(-\sqrt{(Cr-A_{10})t}\right)\right] \quad (22)$$

4. RESULTS AND DISCUSSIONS

In order to attain the perception of the problem, the effects of various parameters encountered into the equations of the problem are studied on primary velocity field (u), secondary velocity field (v), temperature (θ) and concentration field (ϕ) with the help of graphs. Here we consider Gr=Gm=5>0, which corresponds to the cooling plate. The diffusing chemical species of most common interest in air has Schmidt number (*Sc*) and is taken for Hydrogen (*Sc* = 0.22), Helium

(0.30), Steam (0.60).The Prandtl number Pr is taken for air at 20^{o}C (Pr= 0.71).

Extensive computations were performed. Default values of the thermo physical parameters are specified as follows: Rotation parameter K^2=1, Magnetic parameter M = 3, Hall current m =1, Permeability of porous media Kr = 0.5,Phase angle ωt = Pi/2, frequency of oscillations ω = 0.5, Radiation parameter R = 5, Heat source parameter Q = 2, Prandtl number Pr = 0.71(air), Schmidt number Sc = 0.22 (hydrogen), Soret number Sr = 3, Chemical reaction parameter Cr = 0.5 and time t = 1. All graphs therefore correspond to these values unless otherwise indicated.

The effects of governing parameters like rotation, magnetic field, Hall current, thermal bouncy force, concentration buoyancy force, Phase angle , radiation, mass diffusion , thermal diffusion, Soret number, chemical reaction and time on the flow field in the boundary layer region have been presented in the respective Figures 2 to 33.

Figures 2 & 3 indicate the effects of rotation K^2 on the primary and secondary fluid velocities respectively. In particular, from Figures 2 & 3 that primary fluid velocity u decreases whereas secondary fluid velocity v increases on increasing K^2 .

Figures 4 & 5 illustrate the influences of magnetic parameter M. It is noticed from Figures. 4 & 5 that both primary and secondary fluid velocities decreases on increasing M for air (Pr = *0.71*) in presence of Hydrogen. The existence of transverse magnetic field produces a resistive force (Lorentz force) on the fluid flow, this serves to decelerate the flow along the plate in both the primary and secondary flow directions.

Figures 6 to 11 depict the influence of Hall current, thermal and concentration buoyancy forces on the primary and secondary fluid velocities. It is exposed from Figures. 6 to 11 that both primary and secondary fluid velocities increase on increasing either m or Gr or Gm. This implies that Hall current, thermal buoyancy force and concentration buoyancy force tends to accelerate fluid flow in both the primary and secondary flow directions.

Figures 12 & 13 demonstrate the influence of Phase angle ωt on the primary and secondary fluid velocities respectively. It is shown from Figures. 12 & 13 that both primary and secondary fluid velocities decrease on increasing ωt.

Figures 14 & 15 display the effects of the Prandtl number Pr on primary and secondary fluid velocities for cooling of the plate respectively. It is evident from Figures. 14 & 15 that, both the primary and secondary velocity profile decreases on increasing of Pr. The velocity for Pr = 0.71 is higher than that of Pr = 7. Physically, it is possible because fluids with high Prandtl number have high viscosity and hence move slowly in both the primary and secondary flow directions.

Figures 16 to 19 present the effect of thermal Radiation R and Schmidt number Sc the primary and secondary fluid velocities respectively. It is noticed from Figures 16 to 19 that, both primary and secondary velocity profile decreases on increasing of either R or Sc.

The influence of Soret number Sr on Primary and secondary fluid velocities are plotted in Figures 20 & 21.It is noticed from Figures 20 & 21 that both primary and secondary fluid velocities increase on increasing Sr. This implies that Soret number tends to accelerate primary and secondary fluid velocities throughout the boundary layer region.

Figures 22 & 23 depict the influence of chemical reaction parameter Cr on the primary and secondary fluid velocities respectively. It is shown from Figure 22 & 23 that both primary and secondary fluid velocities are decreased on increasing Cr. This implies that chemical reaction tend to slow down fluid flow in both the primary and secondary flow directions.

Figures 24 & 25 present the effect of time t on the primary and secondary fluid velocities. It is evident from Figure 24 & 25 that, u and v increase on increasing t. This implies that, primary and secondary fluid velocities are getting accelerated with the progress of time throughout the boundary layer region.

The numerical solutions for fluid temperature (θ) and species concentration (ϕ) computed from the analytical solutions (17) and (18),are displayed graphically in Figures 26 to 35 for various values of Prandtl number Pr, thermal radiation parameter R, heat source parameter Q, Schmidt number Sc, Soret number Sr and chemical reaction parameter Cr taking t= 1

Figures 26 to 29 illustrates the effect of Prandtl number Pr, heat source parameter Q, Radiation parameter R and time t on fluid temperature. It is evident from Figures 26 to 28 that, fluid temperature decreases on increasing either Pr or Q or R. Figure 29 shows that, there is an enhancement in the temperature of the fluid with the progress of time throughout the thermal boundary layer region.

Figures 30 to 33 shows the effect of various values of the mass diffusion Sc, Soret number Sr, chemical reaction parameter Cr and time t on species concentration. It is noticed from Figures 30 to 33 that, the species concentration increases on increasing of either Sc or t whereas it decreases on increasing of either Sr or Cr.

The numerical values of primary skin friction τ_x and secondary skin friction τ_y ,computed from the analytical expression (22), are presented in Table 1 for various values of K^2, M, m , Gr, Gm, ω, Q, R, Sc, Sr, Cr and t taking Pr = 0.71. It is observed from Table 1 that, the primary skin friction τ_x increases on increasing m, Gr, Gm, ω, Sr and t whereas it decreases increase of K^2, M, Q, R, Sc and Cr. Secondary skin friction increases on increasing of K^2, m, Gr, Gm, ω, Sr and t whereas it decreases increase of M, Q, R, Sc and Cr.

The numerical values of Nusselt number Nu, computed from the equation (20) are presented in Table 2 for different values of Pr, R and Q taking t=1. Table 2 notice that, Nusselt number Nu increases on increasing Pr, Q, R and t.

The numerical values of Sherwood number *Sh*, computed from the analytical expression (21),are displayed in Table 3 for various values of *Pr, R, Sc, Sr* and Cr taking t = 1. It is evident from Table 3 that, the rate of mass transfer increases on increasing of *Pr, R* and *Sr* whereas it decreases on increasing of *Sc* and *Cr*.

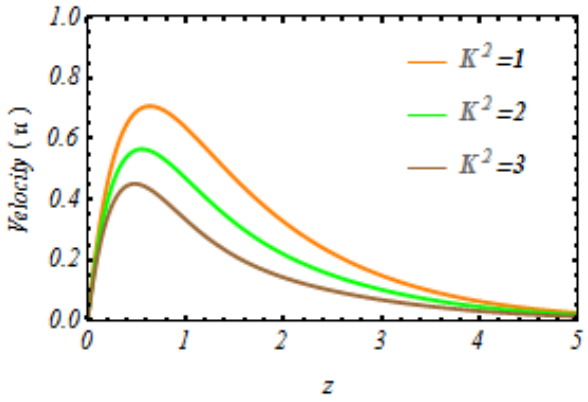

Figure 2: Primary Velocity Profile for Various Values of K^2

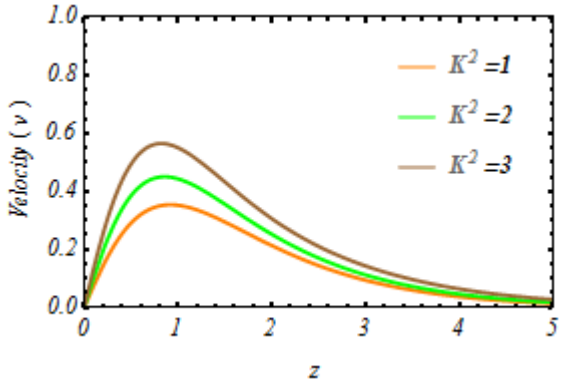

Figure 3: Secondary Velocity Profile for Various Values of K^2

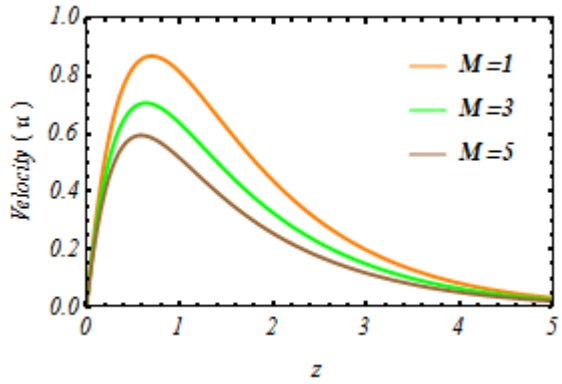

Figure 4: Primary Velocity Profile for Various Values of M

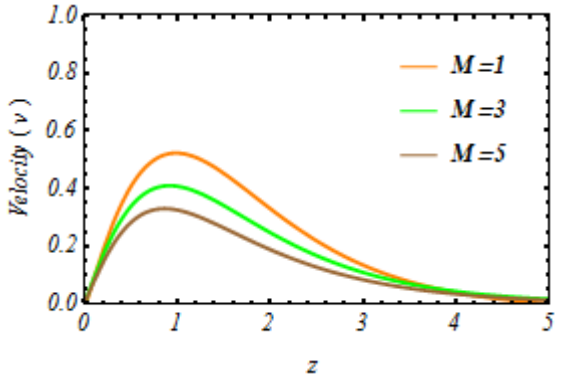

Figure 5: Secondary Velocity Profile for Various Values of M

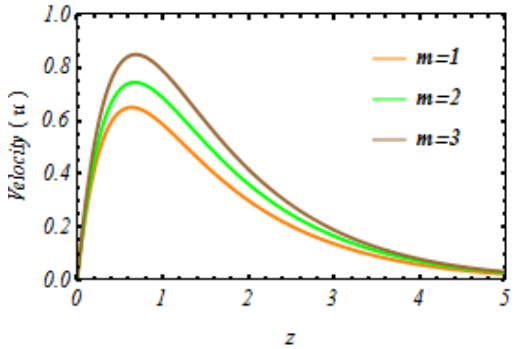

Figure 6: Primary Velocity Profile for Various Values of m

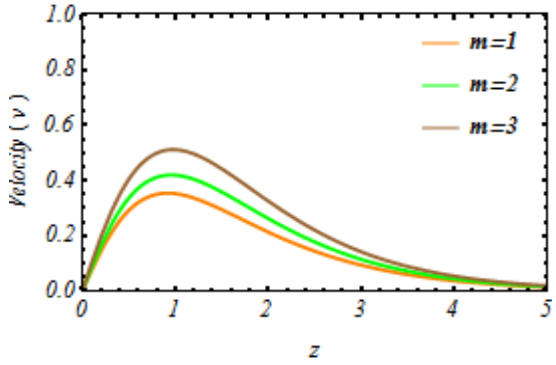

Figure 7: Secondary Velocity Profile for Various Values of m

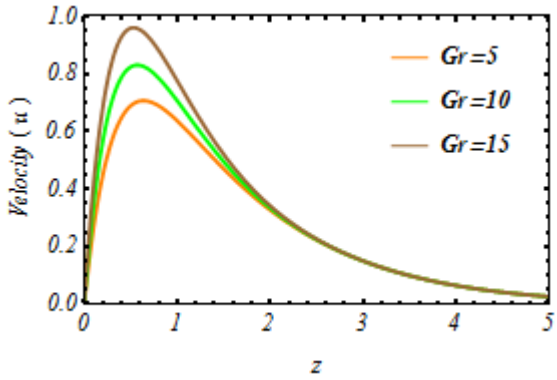

Figure 8: Primary Velocity Profile for Various Values of Gr

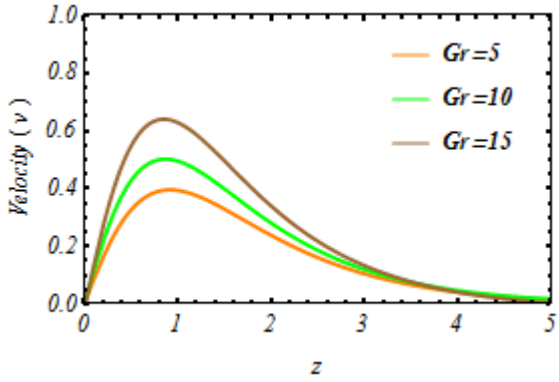

Figure 9: Secondary Velocity Profile for Various Values of Gr

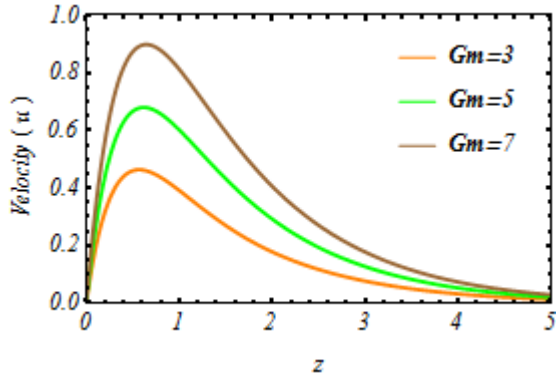

Figure 10: Primary Velocity Profile for Various Values of Gm

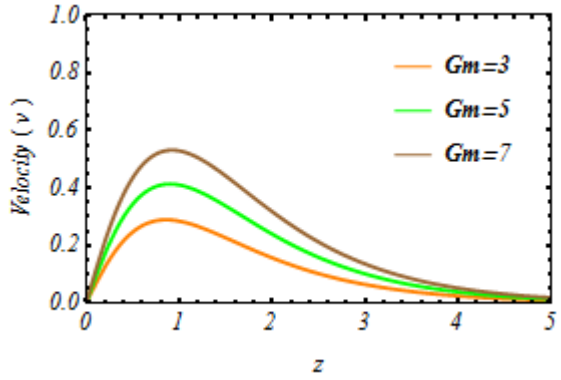

Figure 11: Secondary Velocity Profile for Various Values of Gm

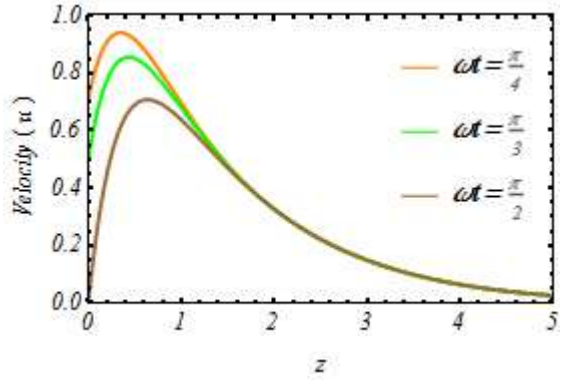

Figure 12: Primary Velocity Profile for Various Values of ωt

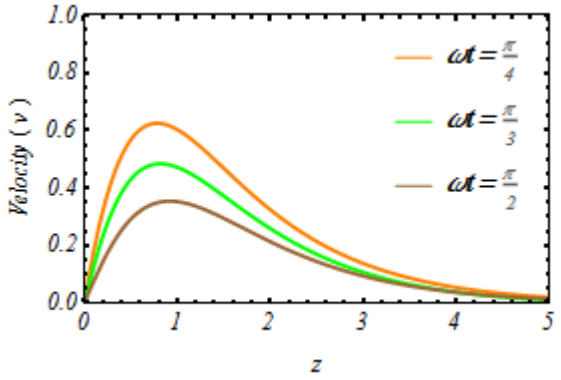

Figure 13: Secondary Velocity Profile for Various Values of ωt

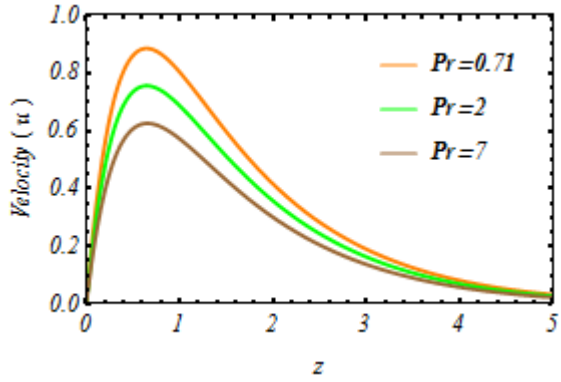

Figure 14: Primary Velocity Profile for Various Values of Pr

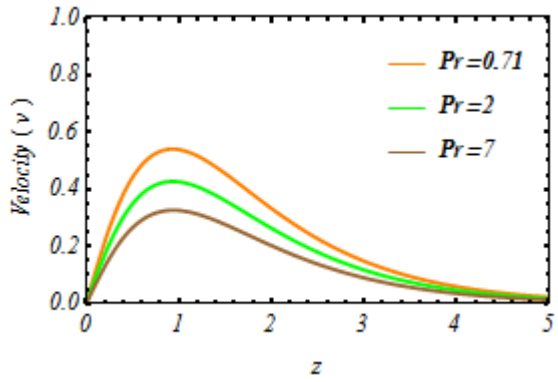

Figure 15: Secondary Velocity Profile for Various Values of Pr

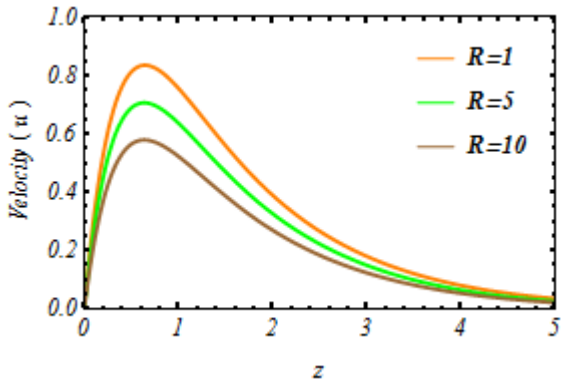

Figure 16: Primary Velocity Profile for Various Values of R

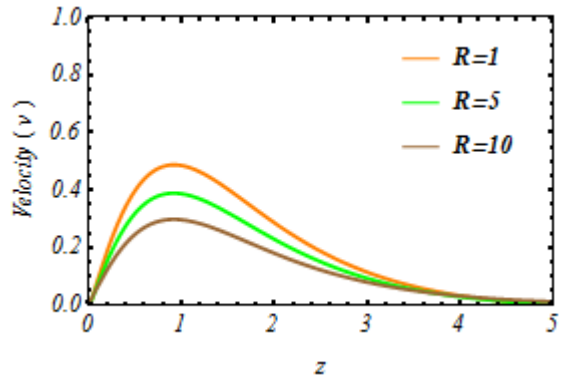

Figure 17: Secondary Velocity Profile for Various Values of R

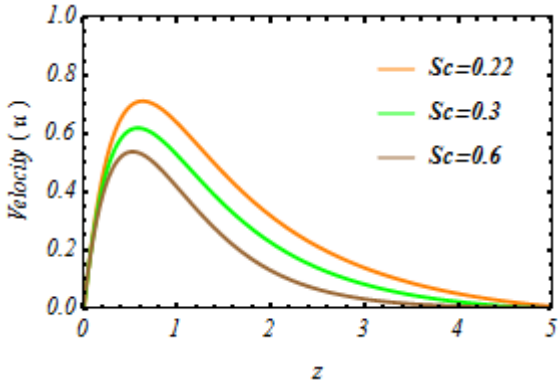

Figure 18: Primary Velocity Profile for Various Values of Sc

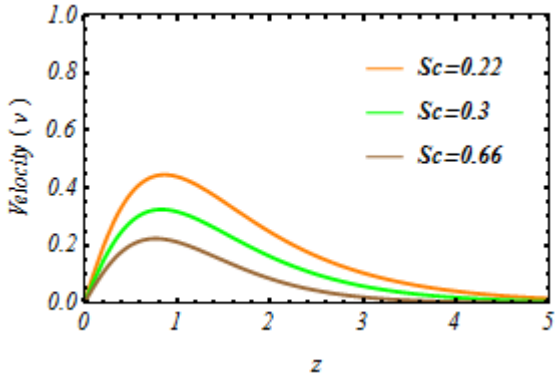

Figure 19: Secondary Velocity Profile for Various Values of Sc

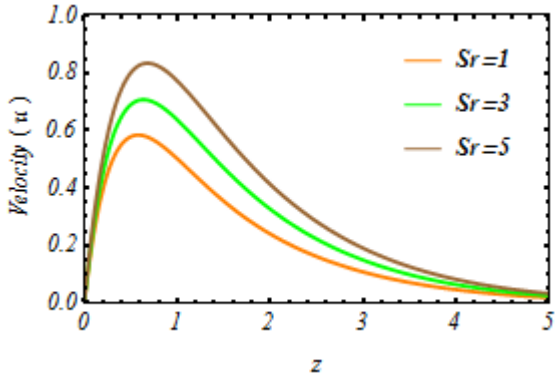

Figure 20: Primary Velocity Profile for Various Values of Sr

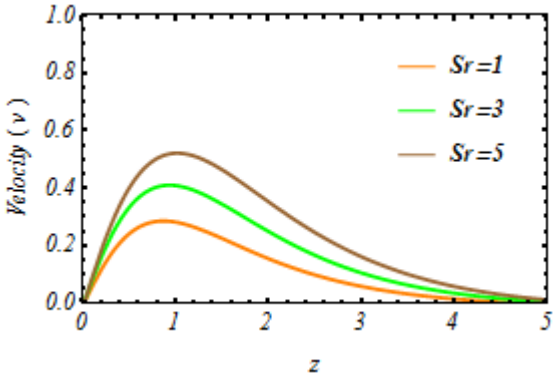

Figure 21: Secondary Velocity Profile for Various Values of Sr

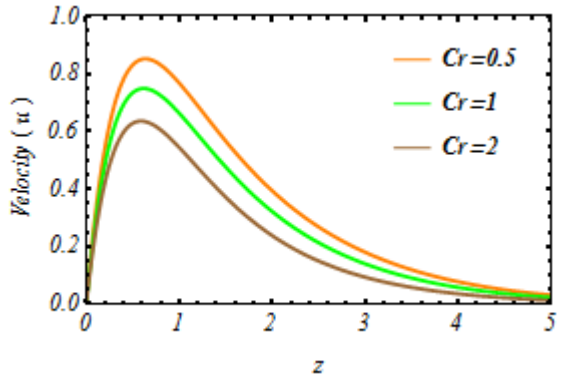

Figure 22: Primary Velocity Profile for Various Values of Cr

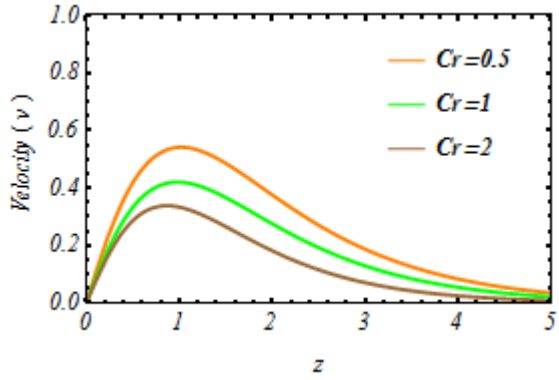

Figure 23: Secondary Velocity Profile for Various Values of Cr

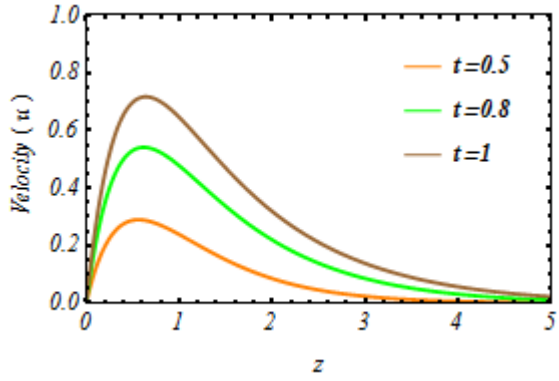

Figure 24: Primary Velocity Profile for Various Values of t

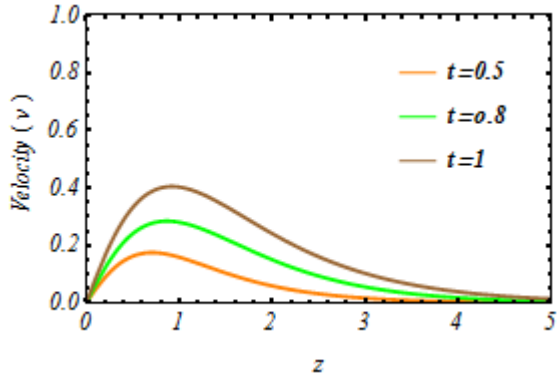

Figure 25: Secondary Velocity Profile for Various Values of t

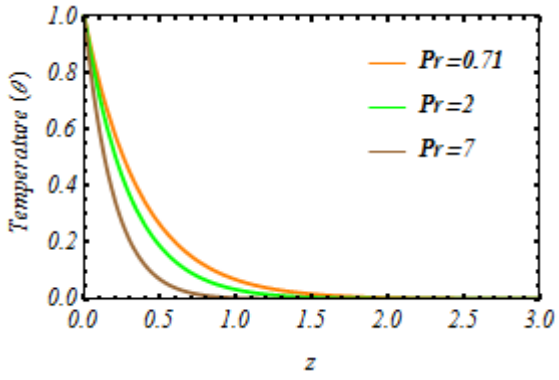

Figure 26: Temperature Profile for Different Values of Pr

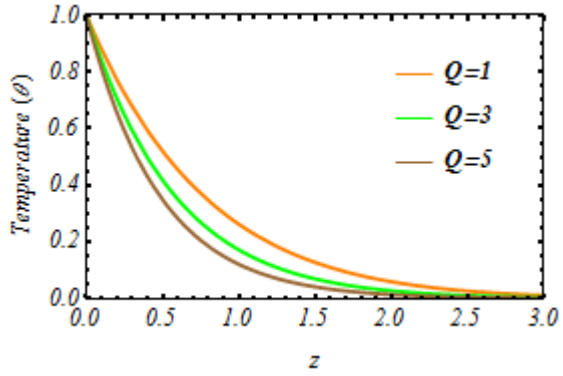

Figure 27: Temperature Profile for Different Values of Q

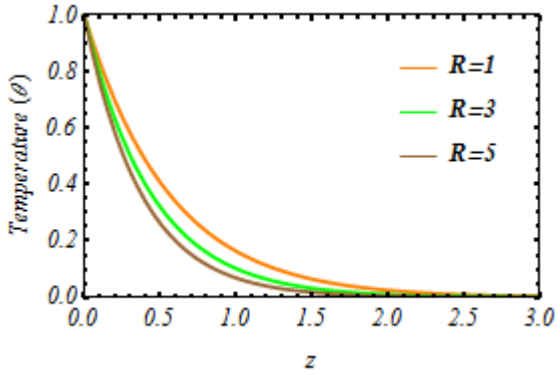

Figure 28: Temperature Profile for Different Values of R

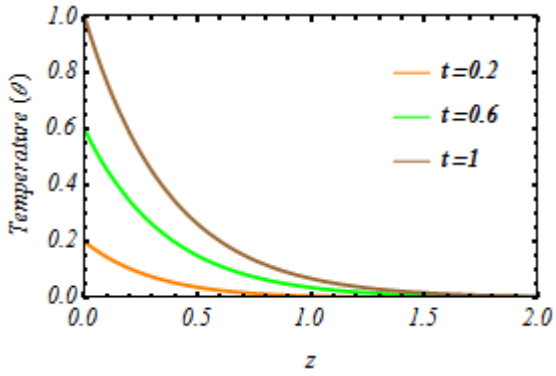

Figure 29: Temperature Profile for Different Values of t

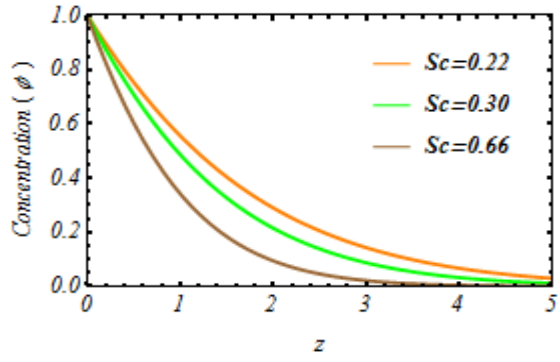

Figure 30: Concentration Profile for Different Values of Sc

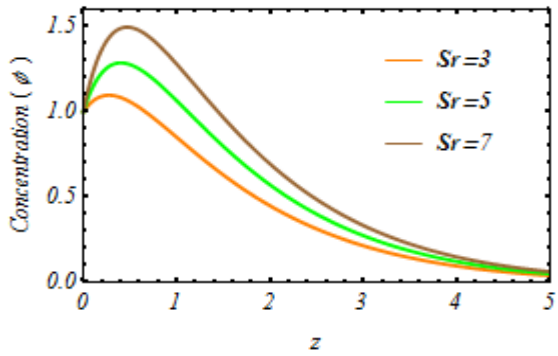

Figure 31: Concentration Profile for Different Values of Sr

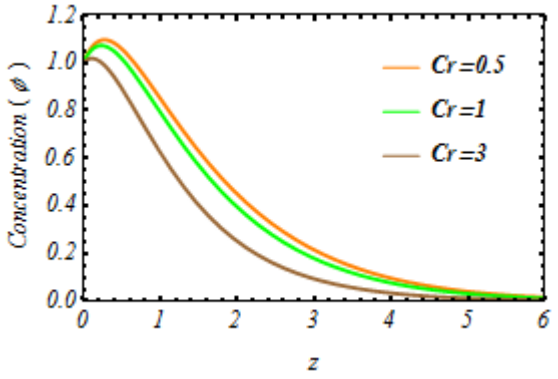

Figure 32: Concentration Profile for Different Values of Cr

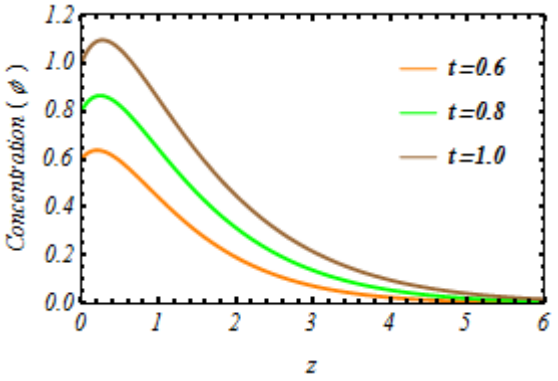

Figure 33: Concentration Profile for Different Values of t

Table 1: Primary Skin Friction (τ_x) and Secondary Skin Friction (τ_y)

K^2	*M*	*m*	*Gr*	*Gm*	*Kr*	*ω*	*Pr*	*Q*	*R*	*Sc*	*Sr*	*Cr*	*t*	τ_x	τ_y
1	3	1	5	5	0.5	0.5	0.71	2	5	0.22	3	0.5	1	**3.13237**	**0.75696**
2	3	1	5	5	0.5	0.5	0.71	2	5	0.22	3	0.5	1	**2.83129**	**0.98749**
1	**5**	**1**	5	5	0.5	0.5	0.71	2	5	0.22	3	0.5	1	**2.86998**	**0.75650**
1	3	**2**	5	5	0.5	0.5	0.71	2	5	0.22	3	0.5	1	**3.33541**	**0.85313**
1	3	1	**7**	5	0.5	0.5	0.71	2	5	0.22	3	0.5	1	**3.52666**	**0.81621**
1	3	1	5	**7**	0.5	0.5	0.71	2	5	0.22	3	0.5	1	**3.94917**	**0.98274**
1	3	1	5	5	**1**	0.5	0.71	2	5	0.22	3	0.5	1	**3.29573**	**0.92628**
1	3	1	5	5	0.5	**1**	0.71	2	5	0.22	3	0.5	1	**3.23658**	**0.79886**
1	3	1	5	5	0.5	0.5	**2**	2	5	0.22	3	0.5	1	**3.08711**	**0.74169**
1	3	1	5	5	0.5	0.5	0.71	**4**	5	0.22	3	0.5	1	**3.11401**	**0.75095**
1	3	1	5	5	0.5	0.5	0.71	2	**10**	0.22	3	0.5	1	**3.07957**	**0.74038**
1	3	1	5	5	0.5	0.5	0.71	2	5	**0.3**	3	0.5	1	**3.20035**	**0.76989**
1	3	1	5	5	0.5	0.5	0.71	2	5	0.22	**5**	0.5	1	**3.42207**	**0.87196**
1	3	1	5	5	0.5	0.5	0.71	2	5	0.22	3	**1**	1	**3.0813**	**0.73402**
1	3	1	5	5	0.5	0.5	0.71	2	5	0.22	3	0.5	**1.5**	**4.83836**	**1.30976**

Table 2: Nusselt Number

Pr	**R**	**Q**	**t**	**Nu**
0.71	5	2	1	2.69733
2	5	2	1	**3.41998**
0.71	**10**	2	1	**3.49301**
0.71	5	**4**	1	**2.94391**
0.71	5	2	**1.5**	**3.95541**

Table 3: Sheerwood Number

Pr	*R*	*Sc*	*Sr*	*Cr*	*Sh*
0.71	5	0.22	3	0.5	0.81763
2	5	0.22	3	0.5	**1.24192**
0.71	**10**	0.22	3	0.5	**1.33751**
0.71	5	**0.3**	3	0.5	**0.65322**
0.71	5	0.22	**5**	0.5	**1.77161**
0.71	5	0.22	3	**1**	**0.70933**

CONCLUSIONS

simultaneous effects of rotation, Soret and Hall current on unsteady hydromagnetic natural convection flow with heat and mass transfer flow of a viscous, incompressible, Newtonian and optically thick radiating fluid past along a vertical oscillating plate with variable temperature and mass diffusion in the presence of transverse magnetic field has been investigated analytically using Laplace transform. The outcomes of the study can be enlisted as:

- Rotation tends to decelerate the primary velocity of the fluid whereas it has a reverse effect on the secondary velocity fluid throughout the boundary layer.
- The primary velocity of the fluid flow increases as increase of Hall current parameter, thermal Grash of number, solutal Grashof number, Soret number and time. However, the primary velocity of the fluid flow was decrease as increase of magnetic parameter, phase angle, Prandtl number, thermal radiation, Schmidt number and chemical reaction.

- The secondary velocity of the fluid flow increases as the current parameter, thermal Grash of number, solutal Grash of number, Soret number and time. However, the secondary velocity of the fluid flow was found to decreases as increase of magnetic parameter, phase angle, Prandtl number, thermal radiation, Schmidt number and chemical reaction.
- Thermal diffusion, thermal radiation and heat source tend to retard the fluid temperature and there is an enhancement in fluid temperature with the progress of time throughout the thermal boundary layer region.
- The concentration profile enhance with increase of Schmidt number and time while on the other hand it responds in an opposite manner with increases of Soret number and Chemical reaction throughout the boundary layer region.
- Rotation tends to decrease the primary skin friction whereas it has reverse effect on secondary skin friction.
- Hall current, thermal buoyancy force, Concentration buoyancy force, frequency of oscillations, Soret number and time has the tendency to enhance the primary and secondary skin frictions .Magnetic field parameter, heat source parameter, radiation parameter, chemical reaction and mass diffusion have the tendency to reduce the primary and secondary skin frictions.
- Thermal diffusion, thermal radiation, heat source parameter and time tend to enhance the rate of heat transfer at the plate.
- Thermal diffusion, thermal radiation and Soret number tend to enhance the rate of mass transfer at the plate whereas mass diffusion and chemical reaction have reverse effect on it.

REFERENCES

1. *Raptis, N.G. Kafoussias, Magnetohydrodynamic free convection flow and mass transfer through porous medium bounded by an infinite vertical porous plate with constant heat flux, Can. J. Phys. 60 (12) (1982) 1725–1729.*
2. *M.A. Sattar, Unsteady hydromagnetic free convection flow with Hall current mass transfer and variable suction through a porous medium near an infinite vertical porous plate with constant heat flux, Int. J. Energy Res. 17 (1993) 1–5.*
3. *Y.J. Kim, Heat and mass transfer in MHD micropolar flow over a vertical moving porous plate in a porous medium, Transp.Porous Media 56 (1) (2004) 17–37.*
4. *B.S. Jaiswal, V.M. Soundalgekar, Oscillating plate temperature effects on a flow past an infinite vertical porous late with constant suction and embedded in a porous medium, Heat Mass Transfer. 37 (2001) 125–131.*
5. *Raptis, C. Perdikis, Unsteady flow through a highly porous medium in the presence of radiation, Transp. Porous Media 57(2004) 171–179.*
6. *S. Ahmed, Free convective transient three-dimensional flow through a porous medium oscillating with time in presence of periodic suction velocity, Int. J. Appl. Math. Mech. 6 (2010) 1–16.*
7. *A.G.V. Kumar, S.V.K. Varma, Thermal radiation and mass transfer effects on MHD flow past a vertical oscillating plate with variable temperature effects variable mass diffusion, Int. J. Eng. 3 (2011) 493–499.*
8. *A.A. Mahmoud, A.J. Chamkha, Non-similar solutions for heat and mass transfer from a surface embedded in a porous medium for two prescribed thermal and solutal boundary conditions, Int. J. Chem. Reactor Eng. 8 (2010) 1–24.*

9. *V.M. Soundalgekar, H.S. Takhar, Radiation effects on free convection flow past a semi-infinite vertical plate, Model. Meas. Control B 51 (1993) 31–40.*
10. *M.A. Hossain, H.S. Takhar, Radiation effect on mixed convection along a vertical plate with uniform surface temperature, Heat Mass Transfer. 31 (1996) 243–248.*
11. *A. Raptis, C. Perdikis, Radiation and free convection flow past a moving plate, Int. J. Appl. Mech. Eng. 4 (1999) 817–821.*
12. *S. Ahmed, Induced magnetic field with radiating fluid over a porous vertical plate: analytical study, J. Naval Archit. Mar.Eng. 7 (2010) 83–94.*
13. *S. Ahmed, K. Kalita, A sinusoidal fluid injection/suction on MHD three-dimensional Couette flow through a porous medium in the presence of thermal radiation, J. Energy Heat Mass Transfer 35 (2012) 41–67.*
14. *S. Ahmed, K. Kalita, Analytical and numerical study for MHD radiating flow over an infinite vertical plate bounded by porous medium in presence of chemical reaction, J. Appl. Fluid Mech. 6(4) (2013) 597–607.*
15. *S. Ahmed, J. Zueco, L.M. Lo´ pez-Ochoa, Numerical modeling of MHD convective heat and mass transfer in presence of first order chemical reaction and thermal radiation, Chem. Eng. Commun. 201 (3) (2014) 419–436, http://dx.doi.org/10.1080/00986445. 2013.775645.*
16. *S. Ahmed, A. Batin, A.J. Chamkha, Finite difference approach in porous media transport modeling for magnetohydrodynamic unsteady flow over a vertical plate: Darcian model, Int. J.Numer. Methods Heat Fluid Flow 24 (5) (2014) 1204–1223, 10.1108/HFF-01-2013-0008.*
17. *S. Ahmed, Numerical analysis for magnetohydrodynamic chemically reacting and radiating fluid past a non-isothermal impulsively started vertical surface adjacent to a porous regime, Ain Shams Eng. J. 5 (2014) 923–933, http://dx.doi.org/10.1016/j.asej. 2014.02.005.*
18. *S. Ahmed, A. Batin, A.J. Chamkha, Numerical/Laplace transform analysis for MHD radiating heat/mass transport in a Darcian porous regime bounded by an oscillating vertical surface, Alexandria Engineering Journal(2015)54,45 54,http://dx.doi.org/ 10.1016/ j.aej. 2014.11.006.*